INTERNATIONAL JOURNAL OF ENERGY RESEARCH
Int. J. Energy Res. 2003; **27**:725–745 (DOI: 10.1002/er.908)

Comparative study between parallel and counter flow configurations between air and falling film desiccant in the presence of nanoparticle suspensions

A. Ali[1], K. Vafai[2,*,†] and A.-R. A. Khaled[1]

[1] *Department of Mechanical Engineering, Ohio State University OSU, Columbus, OH, 43210, U.S.A.*
[2] *Department of Mechanical Engineering, University of California at Riverside UCR, Riverside, CA, 92521, U.S.A.*

SUMMARY

A comparative numerical study is employed to investigate the heat and mass transfer between air and falling film desiccant in parallel and counter flow configurations. Nanoparticles suspensions are added to the falling film desiccant to study heat and mass transfer enhancements. The numerical results show that the parallel flow channel provides better dehumidification and cooling processes of the air than counter flow configuration for a wide range of pertinent parameters. Low air Reynolds number enhances the dehumidification and cooling rates of the air and high air Reynolds number improves the regeneration rate of the liquid desiccant. An increase in the channel height results in enhancing the dehumidification and cooling processes of air and regeneration rate of liquid desiccant. The dehumidification and cooling rates of air are improved with an increase in the volume fraction of nanoparticles and dispersion factor. Copyright © 2003 John Wiley & Sons, Ltd.

KEY WORDS: parallel/counter flow; air flow; falling film desiccant; laminar; nanoparticles suspensions; heat and mass transfer; enhancements; dispersion

1. INTRODUCTION

The use of solid/liquid desiccants has received considerable attention in the past few decades. The liquid desiccant can take the moisture from the surrounding air (dehumidification process) at low temperature and then release this moisture (regeneration process) at high temperature with the surrounding air to provide a continuous process of dehumidification of air and regeneration of liquid desiccant. These processes can be used with the conventional vapour compression cycles, which are called hybrid air-conditioning system in the literature. It was found that the new hybrid system will improve the indoor air quality, reduce energy consumption, and produce an environmentally safe product.

*Correspondence to: Prof. K. Vafai, Department of Mechanical Engineering, University of California at Riverside, Riverside, CA 92521, U.S.A.
† E-mail: vafai@engr.ucr.edu

Contract/grant sponsor: DOD/DARPA/DMEA; contract/grant number: DMEA 90-02-2-0216

Received 19 June 2002
Accepted 16 October 2002

The concept of dehumidification between air and liquid desiccant was initiated in 1955 by Lof. A number of research works have been conducted to develop this concept for an air-conditioning system in order to improve its performance. Park *et al.* (1994) investigated coupled heat and mass transfer between laminar liquid film desiccant and air in cross flow numerically and experimentally. The numerical model was based on finite difference where the axial convection term was approximated by upwind differencing and diffusion terms were expressed by central differencing. It was found that a decrease in the mass flow rate of the air resulted in a better control of the humidity ratio and lower temperature for the air. The numerical results displayed the same trend as the experimental results. Rahmah *et al.* (1998) analysed the flow of laminar liquid film desiccant and air in a parallel flow. The numerical scheme was a combination of control volume method and an iterative algorithm. It was found that an increase in the height of the channel caused a decrease in the exit humidity ratio and temperature for the air. The dehumidification process can be enhanced by decreasing the inlet water concentration in the desiccant solution. Saman and Alizadah (2001) proposed a cross flow plate for dehumidification and cooling. An air stream was dehumidified by spraying liquid desiccant and secondary air stream was cooled by water spraying. The numerical model was based on a control volume for each flow chamber and an iterative method was utilized to satisfy the boundary conditions. It was found that the proposed arrangement was insufficient to bring the humidity and temperature of air to a comfort level, and therefore additional processes for dehumidification and cooling were needed to accomplish this task.

Enhancement of heating and cooling of fluids is essential in many industrial applications. Solid particles have a higher thermal conductivity than fluids by a factor of 1–3 order of magnitudes depending on the type of the solid particles (Eastman *et al.*, 2001). Therefore, the presence of solid particles in a fluid is expected to enhance the thermal conductivity of the solid–liquid mixture, which indeed increases; the heat and mass transfer exchange. The nanoparticle suspension in a fluid referred to as nanofluids in the literature is expected to enhance the heat and mass transfer of the conventional working fluid in many industrial applications. The field of nanofluids is still under development. Choi (1995) studied the enhancement of thermal conductivity of fluids with the presence of nanoparticles. Lee *et al.* (1999) investigated the measurement of thermal conductivity of nanofluids. Xuan and Li (2000) used a hot-wire apparatus to measure the thermal conductivity of nanofluids. A theoretical model was proposed to describe heat transfer performance of nanofluids in a tube while accounting for the dispersion factor. It was found that an increase in the partial volume fraction causes a significant increase in the thermal conductivity of the nanofluids. In a later study, Xuan and Roetzel (2000) proposed two different approaches to calculate the thermal conductivity of the nanofluids. The approaches were: conventional approach where the nanofluids were assumed to be conventional single-phase fluid and modified conventional approach where the dispersion factor was taken into account. The analysis for the dispersion factor was based on the dispersion of thermal conductivity in porous media.

In the literature, the analysis of heat and mass transfer between air and falling film desiccant have been analysed for parallel and cross flow channels. In this work, a comparative study is employed to investigate heat and mass transfer enhancements for dehumidification and cooling processes of air and regeneration rate of liquid desiccant between air and falling film desiccant in parallel and counter flow configurations in terms of the pertinent controlling parameters. In addition, nanoparticles suspensions are added to the falling film desiccant to examine heat and mass transfer enhancements. The pertinent parameters are air/desiccant Reynolds numbers,

height of the channel, volume fraction for the nanoparticles suspension in the falling film desiccant, and the dispersion factor.

2. MATHEMATICAL FORMULATION

Both parallel and counter flow configurations are considered for air and falling film desiccant in the presence of nanoparticle suspensions. The assumptions for this analysis are: the flow is assumed to be laminar and steady state; the thermal properties of the air are constant as well as the falling film desiccant except, for the thermal conductivity of the falling film desiccant; the gravitational force for the air is negligible; the thickness of falling film desiccant is constant; the velocity profile is fully developed for both flow regimes; and thermodynamic equilibrium exits at the interface between air and falling film desiccant.

2.1. Flow in a parallel flow channel

The parallel flow channel between air and falling film desiccant is shown in Figure 1(a).

The governing mass and momentum equations for the air are:

$$\frac{\partial u_a}{\partial x} = 0 \tag{1}$$

$$\frac{\partial p}{\partial x} = \mu_a \left(\frac{\partial^2 u_a}{\partial y^2} \right) \tag{2}$$

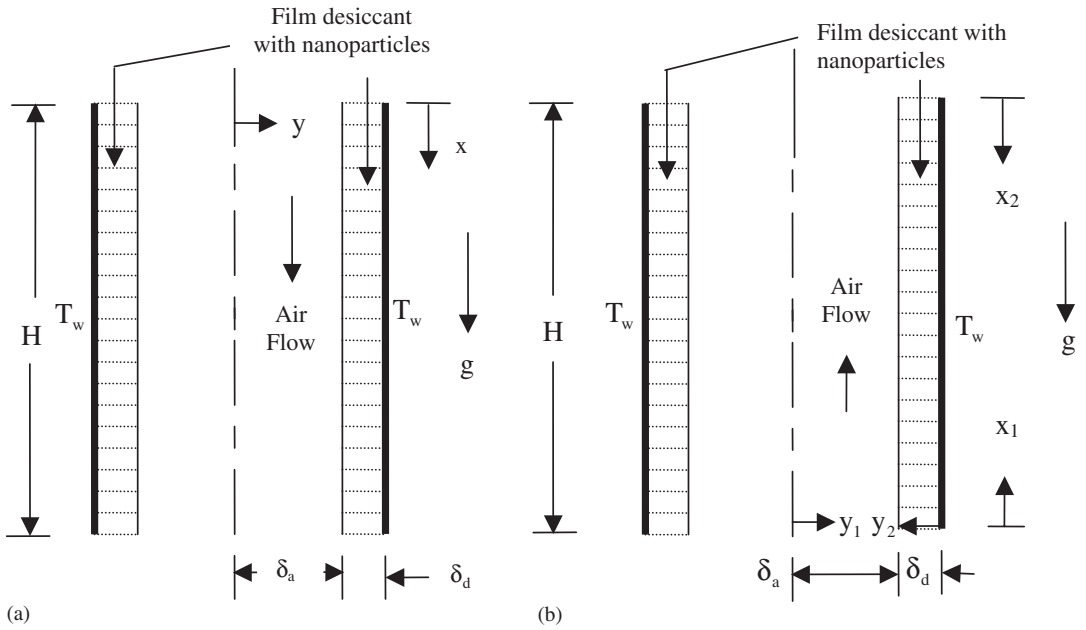

Figure 1. Schematic of vertical channel between air and falling film desiccant (a) parallel flow and (b) counter flow.

The energy equation for the air is

$$\rho_a c_p \left(u_a \frac{\partial T_a}{\partial x} \right) = k_a \frac{\partial^2 T_a}{\partial y^2} \tag{3}$$

The diffusion equation for air can be written as

$$u_a \frac{\partial W}{\partial x} = D_a \left(\frac{\partial^2 W}{\partial y^2} \right) \tag{4}$$

Similarly, the governing mass, momentum, energy and concentration equations for the falling film desiccant are:

$$\frac{\partial u_d}{\partial x} = 0 \tag{5}$$

$$\rho_d g + \mu_d \left(\frac{\partial^2 u_d}{\partial y^2} \right) = 0 \tag{6}$$

$$\rho_d c_p \left(u_d \frac{\partial T_d}{\partial x} \right) = \frac{\partial}{\partial y} \left((k_{eff} + k_{dis}) \frac{\partial T_d}{\partial y} \right) \tag{7}$$

$$u_d \frac{\partial C}{\partial x} = D_d \left(\frac{\partial^2 C}{\partial y^2} \right) \tag{8}$$

The boundary conditions for the parallel flow channel are:

$$T_a = T_{ai}, W = W_i \qquad \text{at } x = 0 \text{ and } 0 \leqslant y \leqslant \delta_a \tag{9}$$

$$T_d = T_{di}, C = C_i \qquad \text{at } x = 0 \text{ and } \delta_a < y \leqslant \delta_a + \delta_d \tag{10}$$

$$\frac{\partial u_a}{\partial y} = 0, \frac{\partial T_a}{\partial y} = 0, \frac{\partial W}{\partial y} = 0 \qquad \text{at } y = 0 \text{ and } 0 \leqslant x \leqslant H \tag{11}$$

$$u_a = u_d, \frac{\partial u_d}{\partial y} = 0, T_a = T_d, W = W_{int} \qquad \text{at } y = \delta_a \text{ and } 0 \leqslant x \leqslant H \tag{12}$$

where W_{int} is the interfacial humidity ratio and is given as (ASHRAE, 1989):

$$W_{int} = 0.62185 \frac{p_z}{(p_t - p_z)} \tag{13}$$

where p_z is equal to (Rahmah *et al.*, 1998):

$$p_z = p_{ws} \left(1.0 - 0.828Z - 1.496Z^2 + Z \frac{(T_{int} - 40)}{350} \right) \tag{14}$$

$$u_d = 0, T_d = T_w, \frac{\partial C}{\partial y} = 0 \qquad \text{at } y = \delta_a + \delta_d \text{ and } 0 \leqslant x \leqslant H \tag{15}$$

The energy balance equation at the interface is

$$-k_a \frac{\partial T_a}{\partial y} - \rho_a D_a h_{fg} \frac{\partial W}{\partial y} = -k_d \frac{\partial T_d}{\partial y} \qquad \text{at } y = \delta_a \text{ and } 0 \leqslant x \leqslant H \tag{16}$$

The mass balance at the interface becomes:

$$-\rho_a D_a \frac{\partial W}{\partial y} = -\rho_d D_d \frac{\partial C}{\partial y} \qquad \text{at } y = \delta_a \text{ and } 0 \leqslant x \leqslant H \tag{17}$$

Analytical solutions are obtained for momentum governing equations for both air and falling film desiccant:

$$u_a(y) = u_{int} - \frac{1}{2\mu_a}\frac{\partial p}{\partial x}\left[\delta_a^2 - y^2\right] \tag{18}$$

$$u_d(y) = \frac{\rho_d g}{2\mu_d}(\delta_a + \delta_d - y) - (y + \delta_d - \delta_a) \tag{19}$$

From the continuity equations for both air and falling film desiccant, the pressure drop in the air and the film thickness of the desiccant can be computed:

$$\frac{\partial p}{\partial x} = \frac{3\mu_a u_{int}}{\delta_a^2} - \frac{3\mu_a \dot{m}_a}{2l\rho_a \delta_a^3} \tag{20}$$

$$\delta_d = \left[\frac{3\dot{m}_d \mu_d}{gl}\right]^{1/3} \tag{21}$$

where $\dot{m}_a$ and $\dot{m}_d$ are mass flow rates of air and desiccant, respectively.

2.2. *Flow in a counter flow channel*

The counter flow channel between air and falling film desiccant are shown in Figure 1(b). The governing equations for momentum, energy, and mass diffusion or concentration for both air and falling film desiccant are the same as the parallel flow arrangement. However since the air will be flowing upward rather than downward, the following boundary conditions will be imposed:

$$T_a = T_{ai}, W = W_i \qquad \text{at } x_1 = 0 \text{ and } 0 \leqslant y_1 \leqslant \delta_a \tag{22}$$

$$T_d = T_{di}, C = C_i \qquad \text{at } x_2 = 0 \text{ and } 0 \leqslant y_2 \leqslant \delta_d \tag{23}$$

$$\frac{\partial u_a}{\partial y_1} = 0, \frac{\partial T_a}{\partial y_1} = 0, \frac{\partial W}{\partial y_1} = 0 \qquad \text{at } y_1 = 0 \text{ and } 0 \leqslant x_1 \leqslant H \tag{24}$$

$$-u_a = u_d, \frac{\partial u_d}{\partial y_2} = 0, T_a = T_d, W = W_{int} \qquad \text{at } y_2 = \delta_d \text{ and } 0 \leqslant x_2 \leqslant H \tag{25}$$

$$u_d = 0, T_d = T_w, \frac{\partial C}{\partial y_2} = 0 \qquad \text{at } y_2 = 0 \text{ and } 0 \leqslant x_2 \leqslant H \tag{26}$$

The energy and mass balance equations at the interface become:

$$-k_a \frac{\partial T_a}{\partial y_1} - \rho_a D_a h_{fg} \frac{\partial W}{\partial y_1} = k_d \frac{\partial T_d}{\partial y_2} \qquad \text{at } y_1 = \delta_a \text{ and } 0 \leqslant x_1 \leqslant H \tag{27}$$

$$-\rho_a D_a \frac{\partial W}{\partial y_1} = \rho_d D_d \frac{\partial C}{\partial y_2} \qquad \text{at } y_1 = \delta_a \text{ and } 0 \leqslant x_1, x_2 \leqslant H \tag{28}$$

The velocity profile and film thickness for the falling film desiccant will be the same as the parallel flow channel. However the velocity profile solution and the pressure drop in the air side will be different:

$$u_a(y_1) = -u_{int} - \frac{1}{2\mu_a}\frac{\partial p}{\partial x}\left[\delta_a^2 - y_1^2\right] \tag{29}$$

$$\frac{\partial p}{\partial x} = -\frac{3\mu_a u_{int}}{\delta_a^2} - \frac{3\mu_a \dot{m}_a}{2l\rho_a \delta_a^3} \tag{30}$$

2.3. Analysis of nanoparticles suspensions in the falling film deisccant

Xuan and Roetzel (2000) proposed two approaches to calculate the thermal conductivity of nanofluids: conventional approach, and the modified conventional approach. The following relationship can be used to calculate $(\rho C_p)_{eff}$ for nanofluids:

$$(\rho c_p)_{eff} = (1-\phi)(\rho c_p)_f + \phi(\rho c_p)_s \tag{31}$$

The volume fraction, ϕ, can be defined as (Xuan and Li, 2000):

$$\phi = \frac{V_s}{V_f + V_s} = N\frac{\pi}{6}d_s^3 \tag{32}$$

Brinkman (1952) extended Einstein's equation for effective fluid viscosity as

$$\mu_{eff} = \mu_f \frac{1}{(1-\phi)^{2.5}} \tag{33}$$

Hamilton and Crosser (1962) developed a relationship for solid–liquid mixture, valid for a conductivity ratio larger than 100:

$$\frac{k_{eff}}{k_f} = \frac{k_s + (n-1)k_f - (n-1)\phi(k_f - k_s)}{k_s + (n-1)k_f + \phi(k_f - k_s)} \tag{34}$$

where

$$n = 3/\psi$$

in which n and ψ are the empirical shape and sphericity of the nanoparticles, respectively. The effective thermal conductivity of nanofluid in Equation (34) is considered for conventional single-phase fluid (conventional approach). Xuan and Roetzel (2000) suggested that the thermal dispersion factor of the nanofluids (modified conventional approach) may be obtained using the dispersed thermal conductivity for a porous medium. There are few suggested forms to calculate the dispersed thermal conductivity in a porous medium (Hunt and Tien, 1988; Plumb, 1983). They can be cast as follows:

$$k_{dis} = C(\rho c\, p)_{eff} u d_s R\phi \tag{35}$$

where C is constant. Amiri and Vafai (1994) found that this constant is a function of:

$$C = f(k_f, \mathrm{Pr}, n) \tag{36}$$

The dispersed thermal conductivity of nanofluid can then be written as

$$k_{dis} = \lambda u \tag{37}$$

where a new constant, λ, is introduced, called dispersion factor, and defined as

$$\lambda = C(\rho c\, p)_{\text{eff}} d_s R\phi \tag{38}$$

Both approaches will be utilized in this study. It should be noted that calcium chloride is used as the falling film desiccant and copper is considered for the nanoparticles suspensions in the falling film desiccant. The moist air is considered as an ideal gas and its properties are taken from ASHRAE handbook of fundamentals (1989), the properties of calcium chloride are obtained from calcium chloride properties handbook (Dow Chemical Company, 1983), and the properties of the copper nanoparticles are obtained from Eastman *et al*. (1997).

2.4. Calculated parameters

The average Nussselt number is defined as follows:

$$\text{Nu}_{\text{AVG}} \equiv \frac{\bar{h}L}{k_a} \equiv \frac{4\delta_a}{H(T_{ai} - T_w)} \int_0^H \left(\frac{\partial T_a}{\partial y}\right)_{y=\delta_a} \mathrm{d}x \tag{39}$$

The average Sherwood number can be written as follows:

$$\text{Sh}_{\text{AVG}} \equiv \frac{\bar{h}_m L}{D_a} \equiv \frac{4\delta_a}{H(W_i - W_{\text{int}})} \int_0^H \left(\frac{\partial W}{\partial y}\right)_{y=\delta_a} \mathrm{d}x \tag{40}$$

The air and desiccant Reynolds number can be cast as

$$\text{Re}_a = \frac{4\rho_a u_{am} \delta_a}{\mu_a} \tag{41}$$

$$\text{Re}_d = \frac{4\rho_d u_{dm} \delta_d}{\mu_d} \tag{42}$$

3. NUMERICAL ANALYSIS

Finite difference approximations are employed to solve the governing equations of energy and mass diffusion or concentration for both air and falling film desiccant in parallel and counter flow channels. The axial convection terms are represented by forward difference approximations and diffusion terms are represented by central difference approximations. Three point's finite-difference equations result in a tridiagonal system of algebraic equations which can be efficiently solved using Thomas Algorithm (Davis, 1968). The discretized equations of the energy and mass diffusion equations for both air and falling film desiccant in parallel and counter flow channels are of the following form:

$$A\Psi_{j-1}^{i+1} + B\Psi_j^{i+1} + AT_{j+1}^{i+1} = F\Psi_j^i$$

where Ψ could be the temperature, concentration or humidity ratio and A, B, and F are constants depending on fluid properties, dimension of the channel, and grid size. An implicit method is used to carry out the solutions for the finite-difference equations and an iterative method is employed to satisfy the interfacial conditions between air and falling film desiccant since Equation (13) is a function of the salt concentration in the liquid desiccant. The following

procedure is implemented in analysing the parallel flow configuration:

a. Assume an interfacial humidity ratio at the second row in the x-direction and then solve for the humidity ratio for this row.
b. Solve for the temperature distribution in the air and the falling film desiccant and then the desiccant concentration for the same row in the x-direction.
c. Calculate the interfacial humidity ratio at the interface from Equation (13) and compare it with the assumed value. If the difference is greater than the convergence criterion, update the assumed humidity ratio and repeat steps a–c.
d. If the difference is less than the convergence criterion, march to the next row in the x-direction and repeat steps a–c.
e. Repeat steps a–d for the whole domain.

The procedure utilized in the analysis of the counter flow channel is revised as follows:

I. Assume interfacial humidity ratio and temperature for the whole domain.
II. Solve for the humidity ratio and concentration of the falling film desiccant by marching for the whole air and desiccant domains.
III. Solve for the temperature in the air and falling film desiccant by marching for the whole air and desiccant domains.
IV. Calculate the interfacial temperature form the energy balance equation. If the maximum error between the calculated interfacial temperature and assumed one for the whole domain is greater than the convergence value, update the assumed interfacial temperature and repeat III–IV.
V. If the maximum error between all the newly calculated interfacial temperature and the corresponding ones from the previous iteration is less than the convergence value, calculate the interfacial humidity ratio from Equation (13) and extract the values for all the discretized fields. If the maximum error criterion is greater than the convergence criterion, update humidity ratio and repeat steps II–V.

Table I shows a comparison between the average Nusselt and Sherwood numbers for the present investigation and the values obtained from Rahamah *et al.* (1998) for regular parallel flow falling film desiccant. The comparison is seen to be good with a maximum deviation is about 5.4% for the Nusselt number and 9.7% for the Sherwood number.

4. RESULTS AND DISCUSSION

A comparative numerical study between parallel and counter flow configurations is employed to investigate the effects of various parameters on heat and mass transfer for the dehumidification and cooling of the air and regeneration of liquid desiccant. In addition, nanoparticles suspensions are added to the falling film desiccant to study heat and mass transfer enhancement for both parallel and counter flow channels. The pertinent parameters are air and desiccant Reynolds numbers, height of the channel, volume fraction, and dispersion factor.

4.1. Effect of air Reynolds number

The impact of air Reynolds number on heat and mass transfer is significant for both parallel and counter flow channels in dehumidification and cooling processes of air. As expected, an increase

Table I. Comparison between Nusselt and Sherwood numbers for the present investigation and Rahamah *et al.* at $Re_a = 1350$, $Re_d = 14$, $T_{ai} = 35°C$, $W_i = 0.02\,kg_w\,kg_a^{-1}$

			Present investigation		Rahamah *et al.*		% error	
H	*L*	*Z*	Nu_{AVG}	Sh_{AVG}	Nu_{AVG}	Sh_{AVG}	Nu_{AVG}	Sh_{AVG}
Dehumidification ($T_w = 10°C$ & $T_{di} = 25°C$)								
0.4	0.0033	0.4	3.04	2.73	2.93	2.50	3.62	8.42
0.5	0.0033	0.4	2.54	2.25	2.45	2.07	3.54	8.00
0.6	0.0033	0.4	2.18	1.91	2.08	1.75	4.59	8.38
0.7	0.0033	0.4	1.89	1.65	1.84	1.51	2.65	8.48
0.4	0.003	0.4	2.79	2.49	2.68	2.25	3.94	9.64
0.4	0.0035	0.4	3.19	2.88	3.08	2.67	3.44	7.29
0.4	0.004	0.4	3.55	3.24	3.44	2.95	3.10	8.95
Regeneration ($T_w = 60°C$ & $T_{di} = 35°C$)								
0.4	0.0033	0.4	3.06	2.46	2.91	2.27	4.90	7.72
0.5	0.0033	0.4	2.55	2.01	2.44	1.88	4.31	6.47
0.6	0.0033	0.4	2.18	1.70	2.08	1.58	4.59	7.06
0.7	0.0033	0.4	1.90	1.46	1.81	1.38	4.74	5.48
0.4	0.003	0.4	2.81	2.21	2.66	2.06	5.34	6.79
0.4	0.0035	0.4	3.22	2.62	3.06	2.40	4.97	8.40
0.4	0.004	0.4	3.59	3.00	3.42	2.73	4.97	9.00

in the air Reynolds number increases the heat and mass transfer rates for the water vapour resulting in an increase in the average Nusselt and Sherwood numbers for both flow configurations, as seen in Figures 2(a) and 2(b). Figure 2(c) illustrates that the exit humidity ratio and air temperature increase with an increase in the air Reynolds number because inlet air conditions convect further out. This indicates that better dehumidification and cooling rates for the air can be achieved at low air Reynolds numbers. In addition, the parallel flow channel provides better performance in dehumidification and cooling processes for the air than the counter flow arrangement. These lower air exit conditions reduce the load in the evaporator section and therefore decrease the overall energy consumption on the air-conditioning system.

The regeneration process is affected by an increase in the air Reynolds number for both types of configurations considered in this work. The average Sherwood number increases with an increase in the air Reynolds number, as seen in Figure 3(a). However, the exit concentration for the liquid desiccant decreases with an increase in the air Reynolds number, as shown in Figure 3(b), for both flow arrangements. Both flows have almost the same exit conditions and therefore the regeneration process is enhanced by both flow configurations.

4.2. *Effect of the desiccant Reynolds number*

The desiccant Reynolds number has a noticeable effect on the dehumidification and cooling processes of the air for both flow regimes. The inlet conditions of the liquid desiccant convect further out with an increase in the desiccant Reynolds number, which results in a decrease in the effective temperature difference between air and liquid desiccant. Therefore, the average Nusselt number decreases for both flow configurations, as shown in Figure 4(a). In the counter flow channel, the humidity ratio starts to increase toward the exit due to the inlet concentration of

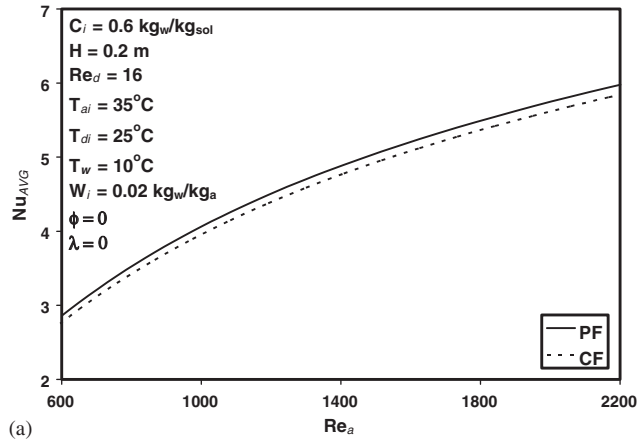

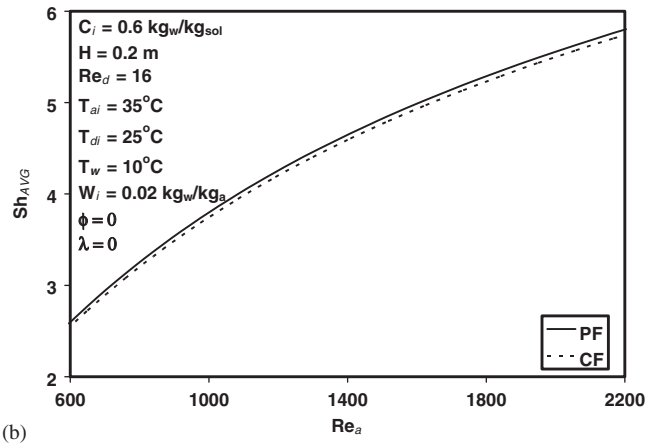

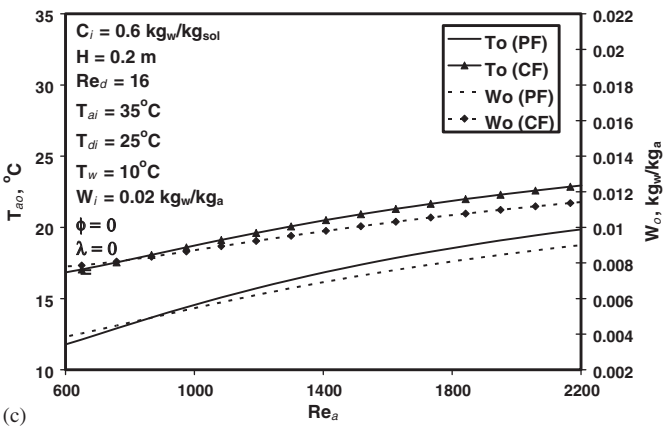

Figure 2. Effect of air Reynolds number for dehumidification and cooling processes of air on (a) average Nusselt number, (b) average Sherwood number, and (c) exit air conditions.

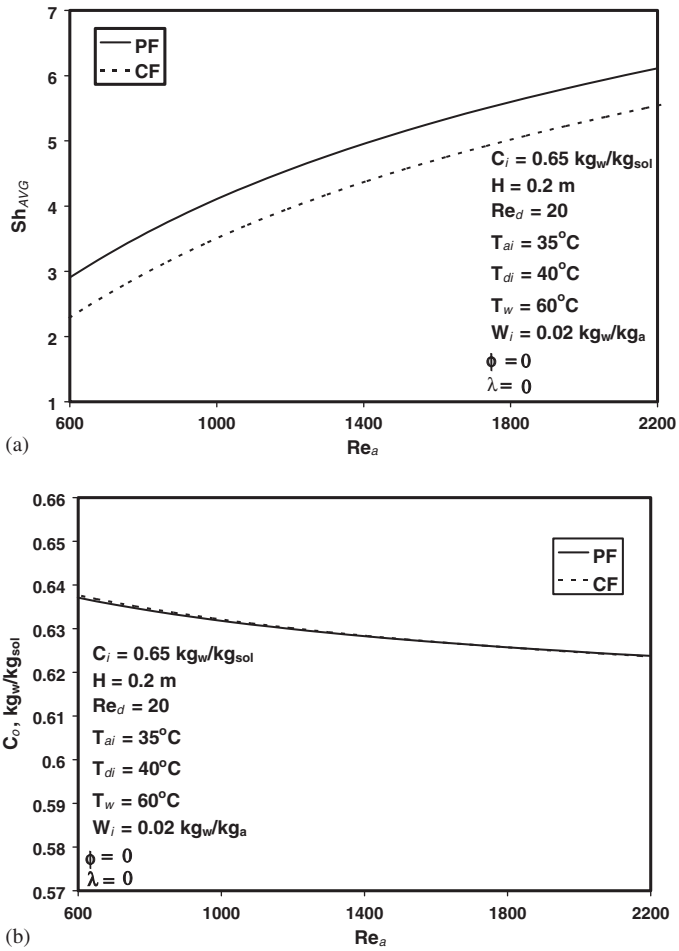

Figure 3. Effect of air Reynolds number for regeneration process of liquid desiccant on (a) average Sherwood number, and (b) exit concentration of liquid desiccant.

the liquid desiccant, which results in a decrease in the effective humidity ratio difference between air and liquid desiccant and the average Sherwood number, as illustrated in Figure 4(b). However, no significant changes are noticed in the average Sherwood number for the parallel flow arrangement. It should be noted that parallel flow channel has a lower exit humidity ratio and air temperature than the counter flow regime because the air will face an additional heating toward the exit as the inlet temperature of the desiccant is higher than the wall temperature in the counter flow arrangement, as illustrated in Figure 4(c). As a result, the parallel flow configuration produces better dehumidification and cooling rates for the air than the counter flow arrangement.

In the regeneration process, the average Sherwood number increases in the parallel flow channel and decreases in the counter flow regime, as seen in Figure 5(a). The exit concentration for the liquid desiccant increases for both flow channels with an increase in the desiccant

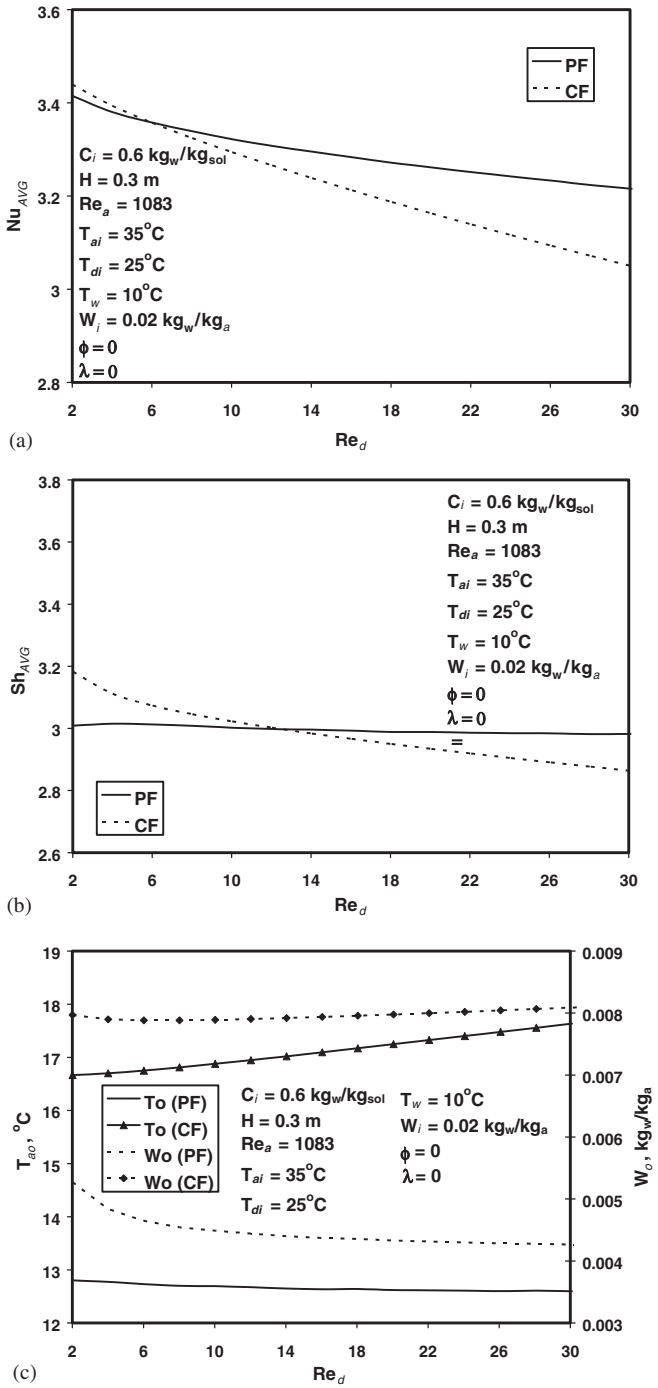

Figure 4. Effect of desiccant Reynolds number for dehumidification and cooling processes of air on (a) average Nusselt number, (b) average Sherwood number, and (c) exit air conditions.

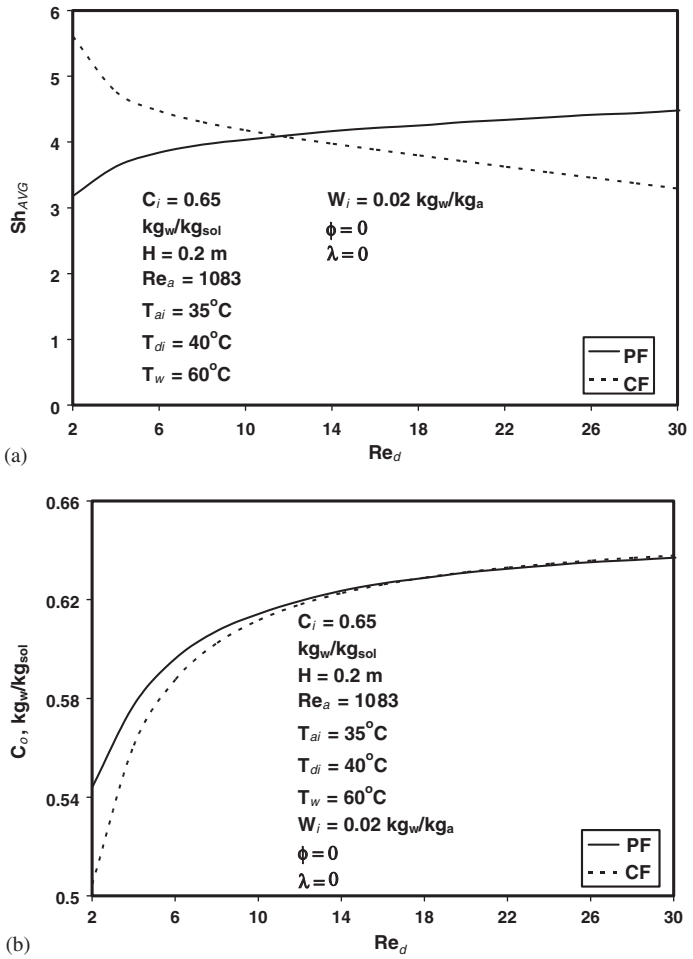

Figure 5. Effect of desiccant Reynolds number for regeneration process of liquid desiccant on (a) average Sherwood number and (b) concentration of liquid desiccant.

Reynolds number, as seen in Figure 5(b). This indicates that low desiccant Reynolds number grants better regeneration process for both configurations as the air will have more time to contact the liquid desiccant at low desiccant Reynolds number. Additionally, the counter flow channel offers better regeneration rates of the liquid desiccant than the parallel flow channel at low desiccant Reynolds number because of lower exit concentration. Better regeneration processes will reduce the overall load on the A/C system and make it more efficient.

4.3. Effect of channel height

Figures 6(c) and 7(b) illustrate the effect of channel height on the exit conditions on air and liquid desiccant for both configurations, respectively. The reduction in the exit conditions for the air and liquid desiccant is dominant at low values of channel height after which the exit

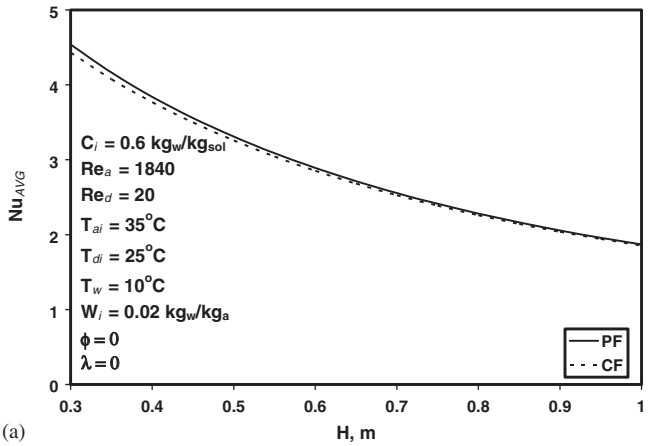

(a)

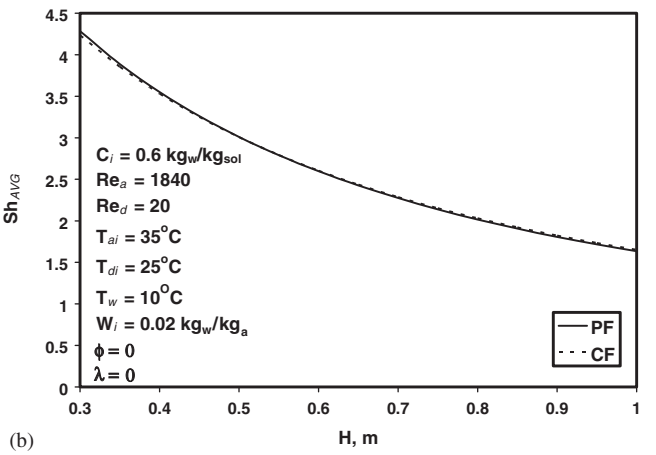

(b)

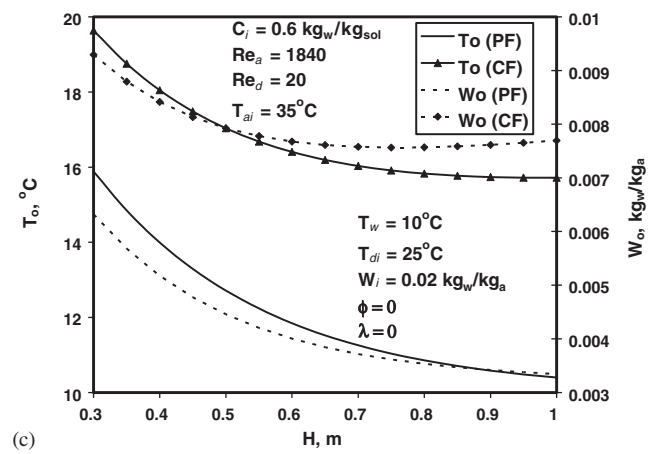

(c)

Figure 6. Effect of channel height for dehumidification and cooling processes of air on (a) average Nusselt number (b) average Sherwood number, and (c) exit air conditions.

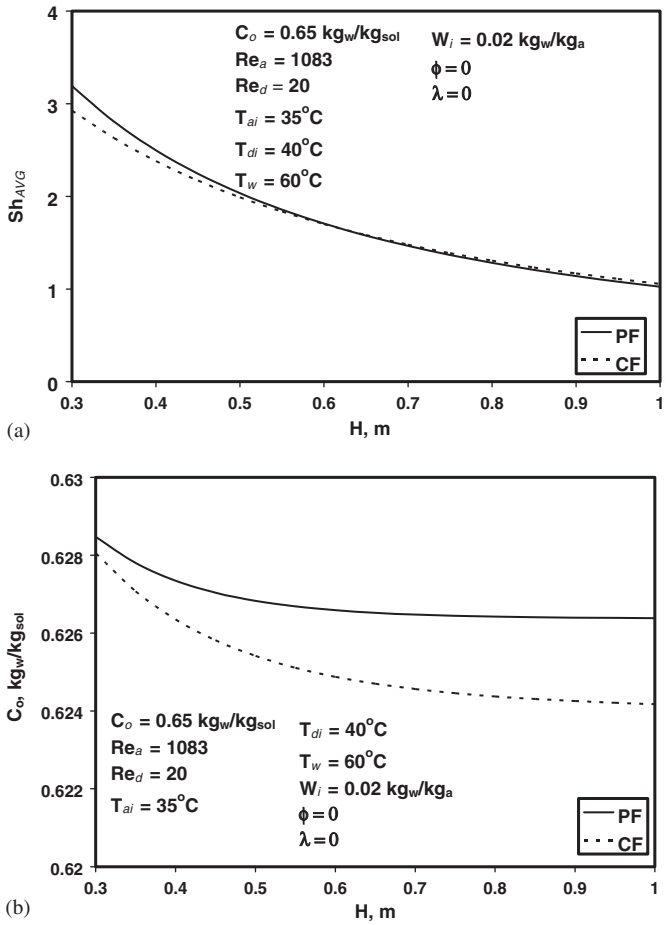

Figure 7. Effect of channel height for regeneration process of liquid desiccant on (a) average Sherwood number, and (b) concentration of liquid desiccant.

conditions reach almost constant values. Regarding the average Nusselt and Sherwood numbers, it is found that they decrease, as seen in Figures 6(a), 6(b) and 7(a), with an increase in the channel height as expected based on Equations (39) and (40).

4.4. Effect of volume fraction

An increase in the volume fraction of the liquid desiccant causes enhancements in the heat transfer at the interface, which in turn increases the average Nusselt number for both flow regimes, as shown in Figure 8(a). An increase in the volume fraction results in an increase in the average Sherwood number for the counter flow configuration yet no significant changes in the average Sherwood number is noticed in the parallel flow arrangement, as seen in Figure 8(b). Exit air conditions decrease with an increase in the volume fraction for both flow configurations, as shown in Figure 8(c), but they are not significant because of the small thickness of the falling

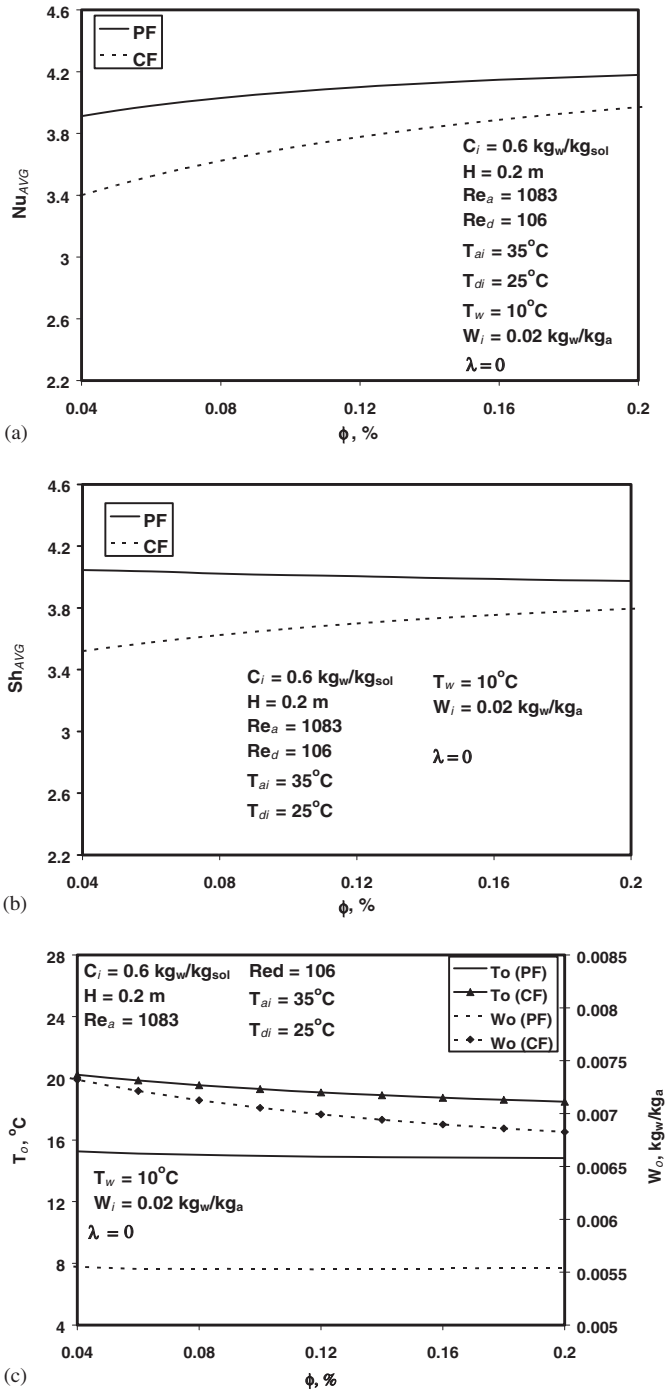

Figure 8. Effect of volume fraction for dehumidification and cooling processes of air on (a) average Nusselt number, (b) average Sherwood number, and (c) exit air conditions.

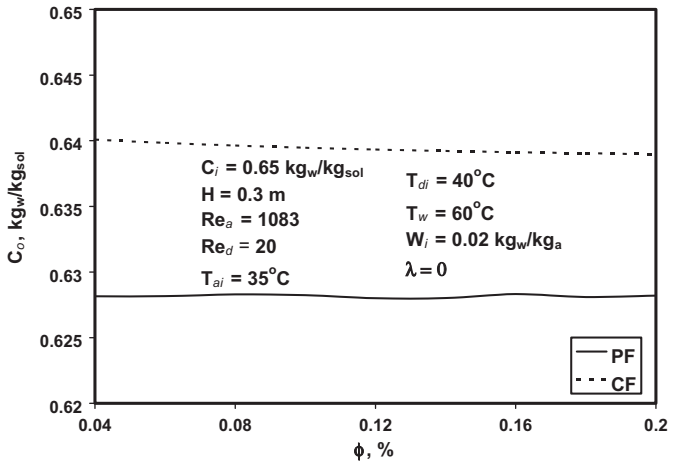

Figure 9. Effect of volume fraction for regeneration process of liquid desiccant on the exit concentration of liquid desiccant.

film desiccant. Additionally, the parallel flow channel provides lower exit conditions which will reduce the overall load on the A/C system.

Figure 9 illustrates that the exit concentration of the liquid desiccant is not affected by an increase in the volume fraction due to the small thickness of the liquid desiccant. Thus, adding nanoparticles suspensions to the falling film desiccant will not improve the regeneration process of the liquid desiccant for either one of the flow configurations.

4.5. Dispersion effects

Due to the presence of nanoparticles suspensions, dispersion factor appears to have an effect in enhancing the heat transfer between air and liquid desiccant at the interface. As expected, an increase in the dispersion factor, λ, causes a slight increase in the average Nusselt number for both flow channels, as seen in Figure 10(a). The average Sherwood number decreases in the parallel flow configuration and increases in the counter flow arrangement with an increase in the dispersion factor, as seen in Figure 10(b). An increase in the dispersion factor causes a decrease in the exit conditions of the air for both flow configurations, as illustrated in Figure 10(c). However, enhancements are not significant due to the small thickness of the film desiccant.

The increase in the dispersion factor has negligible effect on the exit concentration of the liquid desiccant for both flow regimes compared with the volume fraction because the velocity of the desiccant is small, as seen in Figure 11. This indicates that the regeneration process does not get better with an increase in the dispersion factor for either one of the flow configurations.

5. CONCLUSIONS

Enhancements in heat and mass transfer for dehumidification and cooling processes of the air and regeneration of the liquid desiccant in parallel and counter flow configurations are

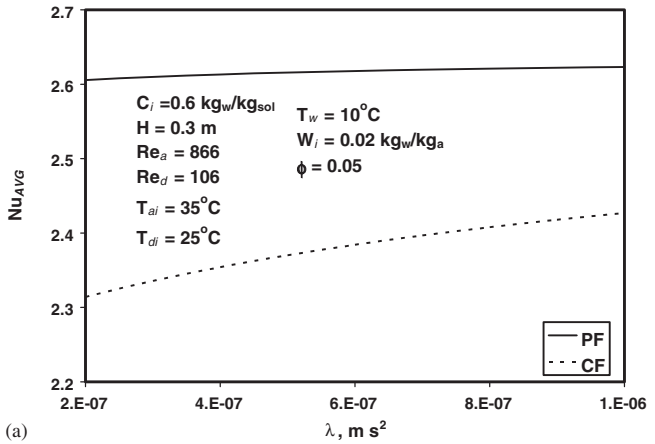

(a)

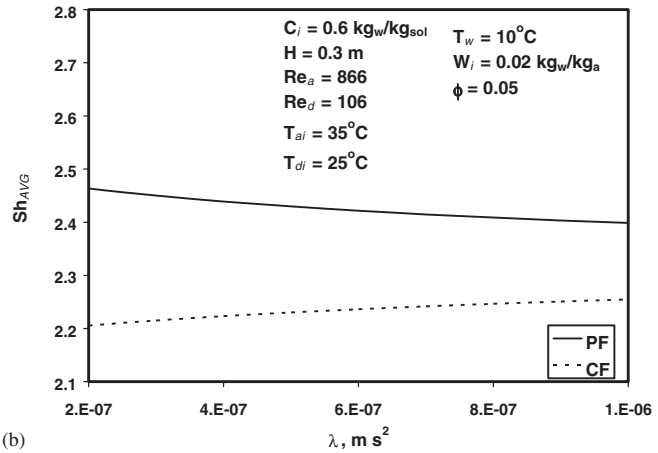

(b)

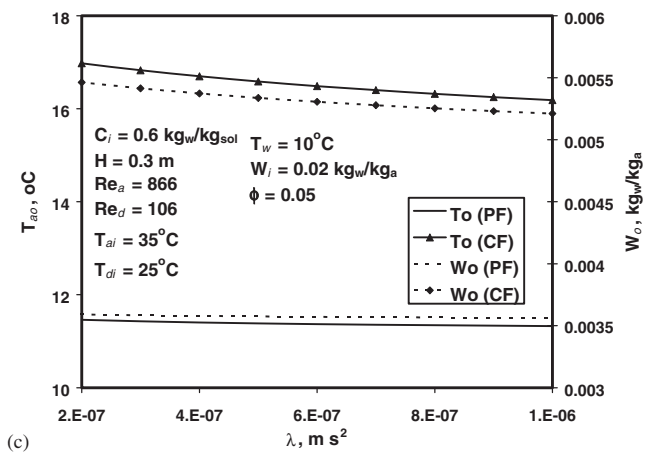

(c)

Figure 10. Effect of dispersion factor for dehumidification and cooling processes of air on (a) average Nusselt number, (b) average Sherwood number, and (c) exit air conditions.

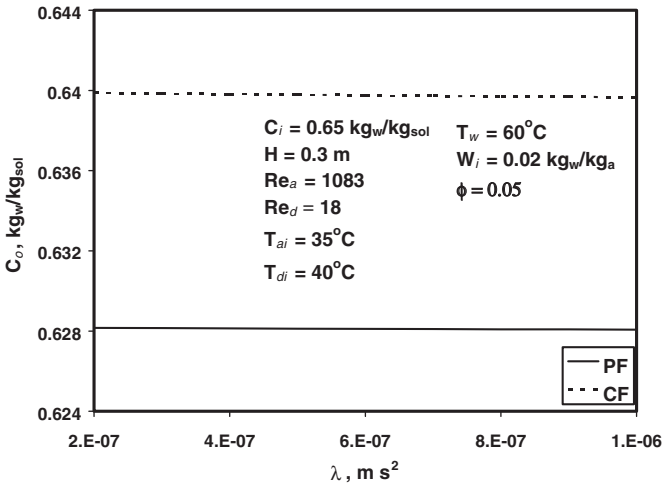

Figure 11. Effect of dispersion factor for regeneration process of liquid desiccant on the exit concentration of liquid desiccant.

investigated in this work. Nanoparticles suspensions are added to the falling film desiccant to study its effect on both of these configurations. Based on the present work, the following attributes were established:

1. The parallel flow channel provides better dehumidification and cooling processes of the air than the counter flow configuration for the entire range of pertinent parameters that were investigated in this work.
2. The counter flow configuration offers better regeneration rate for liquid desiccant than the parallel flow channel in case of varying channel height and low desiccant Reynolds number.
3. Low air Reynolds number enhances the dehumidification and cooling processes of the air for both flow configurations. However, high air Reynolds number improves the regeneration process for the liquid desiccant for both flow configurations.
4. Low desiccant Reynolds number provides better regeneration rates for the both flow configurations.
5. An increase in the height of the channel enhances the dehumidification and cooling rates of the air and the regeneration process of the liquid desiccant for both flow arrangements.
6. The volume fraction and dispersion factor enhance the dehumidification and cooling processes of the air, but the improvements are not significant due to the small thickness of the falling film desiccant.

ACKNOWLEDGEMENT

We acknowledge partial support of this work by DOD/DARPA/DMEA under grant number DMEA90-02-2-0216.

NOMENCLATURE

C	concentration of liquid desiccant ($kg_w\,kg_{sol}^{-1}$)
D	diffusion coefficient ($m^2\,s^{-1}$)
d_s	average diameter of naoparticles (nm)
h	average heat transfer coefficient ($W\,m^{-2}\,^\circ C^{-1}$)
G	gravitational acceleration ($m\,s^{-2}$)
h_m	average mass transfer coefficient ($kg\,m^{-2}\,s^{-1}$)
H	channel height (m)
K	thermal conductivity ($w\,m^{-2}\,^\circ C$)
$\dot{m}$	mass flow rate ($kg\,s^{-1}\,m^{-1}$)
N	number of nanoparticles per unit volume
Nu_{AVG}	average Nusselt number
p_t	total pressure (pa)
p_{ws}	saturation pressure of water vapour (pa)
p_z	vapor pressure of liquid desiccant (pa)
Re	Reynolds number
T	temperature ($^\circ C$)
Sh_{AVG}	average Sherwood number
V	volume (m^3)
W	humidity ratio of the air ($kg_w\,kg_a^{-1}$)
X	x-co-ordinate
Y	y-co-ordinate
Z	salt concentration in the falling film desiccant ($kg_{salt}\,kg_{sol}^{-1}$)

Greek letters

ρ	density ($kg\,m^{-3}$)
δ	thickness (m)
ϕ	volume fraction (%)
λ	dispersion factor ($m^2\,s$)
μ	dynamic viscosity ($N\,s\,m^{-2}$)

Indices

A	air
CF	counter flow
D	desiccant
F	fluid
I	inlet conditions
int	interfacial condition between air and falling film desiccant
M	mean value
O	outlet condition
PF	parallel flow
S	solid
sol	desiccant liquid solution

REFERENCES

Amiri A, Vafai K. 1994. Analysis of dispersion effects and non-thermal equilibrium non-Darcian variable porosity incompressible flow through porous medium. *International Journal of Heat & Mass Transfer* **37**:939–954.

ASHRAE Handbook, *Fundamentals*. 1989. American Society of Heating, Refrigeration, and Air-Conditioning Engineers, Inc.

Brinkman HC. 1952. Viscosity of concentrated suspensions and solutions. *Journal Chemistry Physics* **20**:571–581.

Choi S. 1995. Enhancing thermal conductivity of fluids with nanoparticles. *ASME FED*. **231**:00–103.

Davis RT. 1968. The hypersonic fully viscous shock-layer problems. Report, *SC-RR-68-840*, Sanndia Laboratories.

Dow Chemical Company. 1983. *Calcium Chloride Properties and Forms Hanbook*. Dow Chemical Company, U.S.A.

Eastman JA, Choi US, Li S, Thompson LJ, Lee S. 1997. In *Nanocrystalline and Nanocomposite Materials II*, (vol. 457). Komarnenl S, Parker JC, Wollenberger HC (eds). (Materials Research Society: Pittsburgh PA; 3–11.

Eastman JA, Choi SU, Yu W, Thompson LJ. 2001. Anomalously increased effective thermal conductivities of ethylene glycol-based nanofluids containing copper nanoporticles. *Applied Physics Letters* **78**(5):718–720.

Hamilton RL, Crosser OK. 1962. Thermal conductivity of heterogeneous two-component system. *I&EC Fundamentals* **1**: 182–191.

Hunt ML, Tien CL. 1988. Effect of thermal dispersion on forced convention in fibrous media. *International Journal of Heat and Mass Transfer* **31**:301–309.

Lee S, Choi US, Li S, Eastman JA. 1999. Measuring thermal conductivity of fluids containing oxide nanoparticles *Journal of Heat Transfer* **121**:280–289.

Lof GO. 1955. House heating and cooling with solar energy. *Solar Energy Research*. University of Wisconsin, Madison, USA.

Park MS, Howell JR, Vliet GC, Peterson J. 1994. Numerical and experimental results for coupled heat and mass transfer between a desiccant film and air in cross flow. *International Journal of Heat & Mass Transfer* **37**:395–402.

Plumb OA. 1983. The effect of thermal dispersion on heat transfer in packed bed boundary layers. *Proceedings of the ASME JSME Thermal ENG. Joint conference 2*. 17–22.

Rahmah A, Elsayed AM, Al–Najem NM. 1998. A numerical solution for cooling and dehumidification of air by a falling desiccant film in parallel flow. *Renewable Energy* **13**(3):305–322.

Saman WY, Alizadaeh S. 2001. Modeling and performance analysis of a cross-flow type plate heat exchanger for dehumidification/cooling. *Solar Energy* **70**(4):361–372.

Xuan Y, Li Q. 2000. Heat transfer enhancement of nanofluids. *International Journal Heat and Fluid Flow* **21**:58–64.

Xuan Y, Roetzel W. 2000. Conceptions for heat transfer correlation of nanofluids. *International Journal of Heat Mass and Mass Transfer* **43**:3701–3707.

